

Supporting information

Unravelling the gas condition-dependent aggregation and fragmentation of atomically dispersed Pt catalyst on ceria support

Haodong Wang,^a Hyuk Choi,^b Ryuichi Shimogawa,^{a,c} Yuanyuan Li,^d Lihua Zhang,^e Hyunyou Kim^b and Anatoly I. Frenkel^{*a,f}

a. Department of Materials Science and Chemical Engineering, Stony Brook University, Stony Brook, NY 11794, United States

b. Department of Materials Science and Engineering, Chugman National University, Daejeon 34134, Republic of Korea

c. Mitsubishi Chemical Corporation, Science and Innovation Center, Yokohama 227-8502, Japan

d. Chemical Sciences Division, Oak Ridge National Laboratory, Oak Ridge, TN 37831, United States

e. Center for Functional Nanomaterials, Brookhaven National Laboratory, Upton, NY 11973, United States

f. Division of Chemistry, Brookhaven National Laboratory, Upton, NY 11973, United States

Content

1. Sample Preparation and Characterization

Sample Preparation

Diffuse reflectance infrared Fourier-transform spectroscopy (DRIFTS)

X-ray absorption spectroscopy (XAS)

High Angle Annular Dark Field – Scanning Transmission Electron Microscopy (HAADF-STEM)

2. DFT calculations

3. Supplementary Figures

Figure S1. HAADF-STEM images of the Pt/ceria sample (a) as prepared and (b) after RWGS reaction.

Figure S2. Fourier transform magnitudes of the k^2 -weighted EXAFS data and theoretical (FEFF) fits of the pre-reaction (a) and post-reaction (b) states of the experiment, measured at room temperature.

Figure S3. The DFT-constructed models of (a) CeO₂ (100), (b) Pt₉ Nanocluster, and (c) Pt₁ single atom

Figure S4. The DFT-calculated binding energy, E_{bind} of H_2 on CeO_2 , H_2 on Pt_1/CeO_2 , and CO_2 on Pt_1/CeO_2 .

Figure S5. The DFT-calculated diffusion barrier of the H atom along the CeO_2 (100)

Figure S6. The DFT-estimated interatomic distances of Pt-O, Pt-Pt over the $\text{Pt}_9/\text{H-CeO}_2$, and $9\text{CO}^*-\text{Pt}/\text{H-CeO}_2$

1. Sample Preparation and Characterization

Sample Preparation

Pt/ceria sample was prepared by dispersing 0.5 g cerium (IV) oxide nanopowder (<25 nm) in a solution of 0.42 g of cerium (III) nitrate hexahydrate, 2.0 g urea, and 8 mL of water. The weight loading of Pt was controlled by adding the desired amount of Pt precursor solution (chloroplatinic acid hydrate in water, approximately 1 wt.% Pt). All chemicals were purchased from Sigma-Aldrich. Ultrapure water was provided by Millipore purification system. The mixture was sealed in a glass vial and stirred for 24 hours in an oil bath at 90 °C. Afterward, the samples were washed with deionized water and centrifuged three times. After drying overnight in an oven at 80 °C, the sample was crushed into powders and calcined at 500 °C (5 °C/min heating ramp) for 5 h. The resulting platinum loading of the Pt/ceria sample was measured by inductively coupled plasma optical emission spectrometry (ICP-OES) by Galbraith Laboratories. The instrument measures characteristic emission spectra by optical spectrometry and describes multi-elemental determinations.

Diffuse reflectance infrared Fourier-transform spectroscopy (DRIFTS)

The spectra were collected using an iS50 FTIR spectrometer equipped with a rapid-scanning liquid-nitrogen-cooled mercury cadmium telluride (MCT) detector and a Praying Mantis High Temperature Reaction Chamber (Harrick Scientific Products). Prior to measurement, each sample was heated at 150 °C for 30 minutes under He with a flow rate of 20 ml/min to remove surface adsorbed species followed by collection of background spectra at each temperature. The sample was then cooled to room temperature. The sample was exposed to a mixture of 5% CO_2 and 5% H_2 (balanced with He, with a total flow rate of 31.5 ml/min) at 300 °C to collect reaction spectra. After that, the sample was cooled down to room temperature and collected RT spectra. For cooling down at CO, a mixture of 5% CO (balanced with He, the flow rate is 31.5 ml/min) and He with a flow rate of 10 ml/min was flowed through the reaction chamber for 30 minutes to acquire CO adsorption spectra.

X-ray absorption spectroscopy (XAS)

XAS measurements were performed at the QAS beamline (7-BM) of National Synchrotron Light Source II (NSLS II), Brookhaven National Laboratory. For in-situ measurement, the sample was prepared in a pellet using a hydraulic press and mounted in a Nashner-Adler cell. In-situ data were collected before the reaction, at the reaction condition (5% CO_2 +5% H_2 , 300 °C), and room temperature (5% CO_2 +5% H_2). At each regime, 30 scans of XAS data at the Pt L_3 edge were collected in fluorescence mode.

High Angle Annular Dark Field – Scanning Transmission Electron Microscopy (HAADF-STEM)

HAADF-STEM imaging was carried out on Hitachi HD2700 STEM equipped with a probe aberration corrector, at Center for Functional Nanomaterials, Brookhaven National Laboratory. The powder sample was deposited onto a 3mm Cu grid covered with a ultra-thin carbon layer.

2. DFT calculations

We optimized the $\text{CeO}_2(100)$ surface using a 4×4 supercell with two O-Ce-O layers to describe the ceria nanodomains in the experimental catalyst system, as in our previous results.¹ The vacuum layer was applied to 15 \AA to avoid electronic interference between the periodic supercells. We performed spin-polarized DFT calculations using a plane-wave basis with the VASP code² and the Perdew-Burke-Ernzerhof (PBE)³ of functional. The DFT+U scheme⁴ with $U_{\text{eff}} = 4.5 \text{ eV}$ ^{5,6} was applied for Ce ions to appropriately consider the localized Ce-f orbitals. The projector-augmented wave method⁷ described the interaction between the ionic core and the valence electrons. Valence electron wave functions were expanded on a plane-wave basis up to an energy cutoff of 400 eV. The Brillouin zone was sampled at the Γ -point for all calculations. The convergence criteria for the electronic structure and the atomic geometry were 10^{-4} eV and 0.03 eV/\AA , respectively. We used a Gaussian smearing function with a finite temperature width of 0.05 eV to improve the convergence of states near the Fermi level. The location and energy of transition states (TSs) were calculated with the climbing-image nudged-elastic-band method.⁸

4. Supplementary Figures

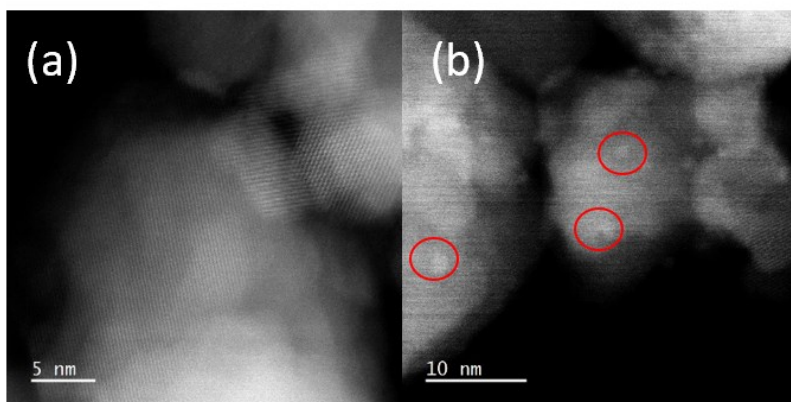


Figure S1. HAADF-STEM images of the Pt/ceria sample (a) as prepared and (b) after RWGS reaction.

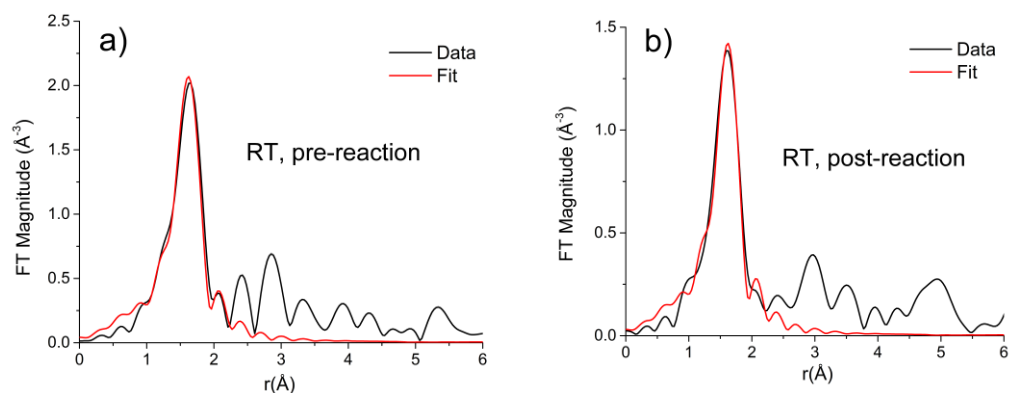


Figure S2. Fourier transform magnitudes of the k^2 -weighted EXAFS data and theoretical (FEFF) fits of the pre-reaction (a) and post-reaction (b) states of the experiment, measured at room temperature.

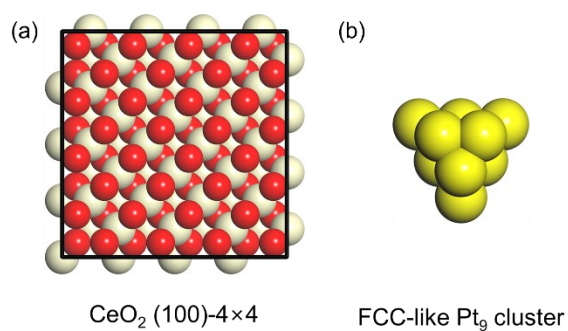


Figure S3. The DFT-constructed models of (a) CeO_2 (100) and (b) Pt_9 nanocluster.

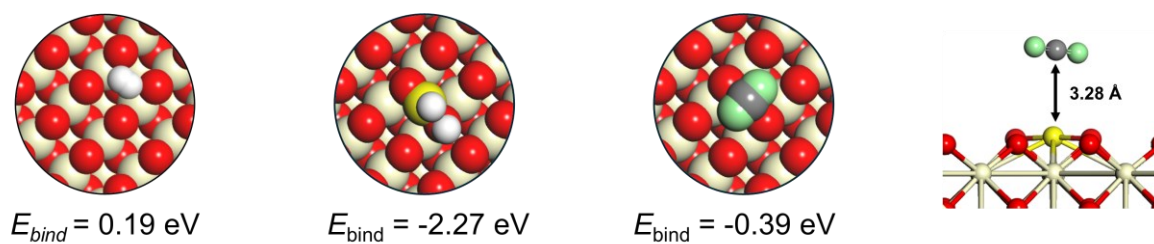


Figure S4. The DFT-calculated binding energy, E_{bind} of H_2 on CeO_2 (0.19 eV), H_2 on Pt_1/CeO_2 (-2.27 eV), and CO_2 (-0.39 eV) on Pt_1/CeO_2 .

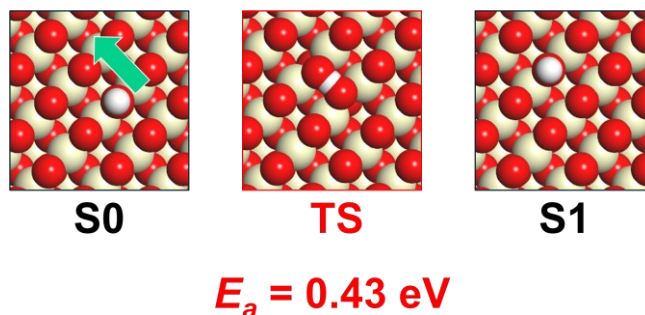


Figure S5. The DFT-calculated diffusion barrier of the H atom along the CeO₂ (100).

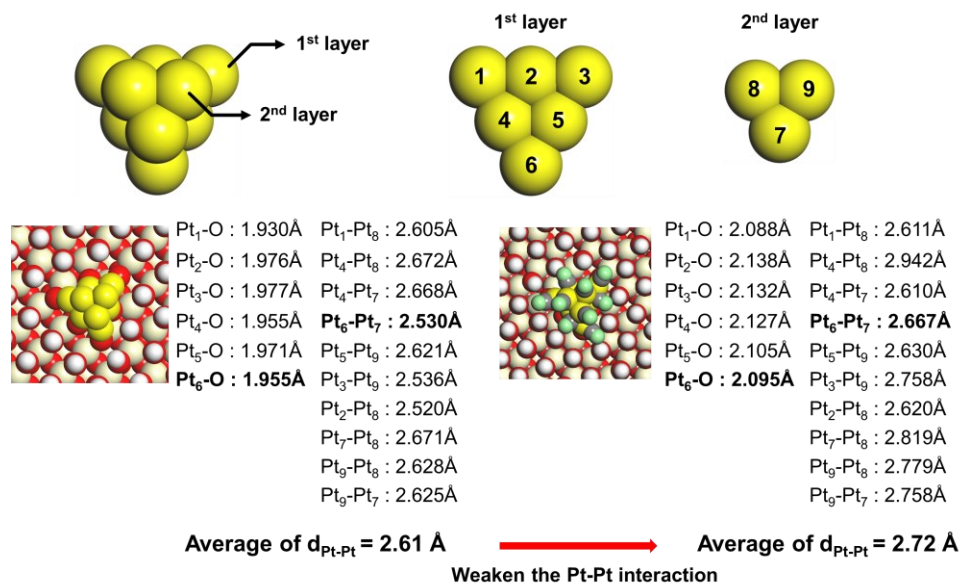


Figure S6. The DFT-estimated interatomic distances of Pt-O and Pt-Pt over the Pt₉/H-CeO₂, and 9CO*-Pt/H-CeO₂.

References

1. M. Kottwitz, Y. Li, R. M. Palomino, Z. Liu, Q. Wu, G. Wang, J. Huang, J. Timoshenko, S. D. Senanayake, M. Balasubramanian, D. Lu, R. G. Nuzzo, A. I. Frenkel, *ACS. Catal.*, 2019, 9, 8738-8748.
2. G. Kresse and J. Furthmüller, *Comp. Mater. Sci.* 1996, **6**, 15-50
3. J. P. Perdew, K. Burke and M. Ernzerhof, *Phys. Rev. Lett.* 1996, **77**, 3865-3868.
4. S. I. Dudarev, G. A. Botton, S. Y. Savrasov, C. J. Humphreys and A. P. Sutton, *Phys. Rev. B* 1998, **57**, 1505-1509.
5. H. Y. Kim, M. S. Hybertsen and P. Liu, *Nano Lett.* 2017, **17**, 348-354

6. M. Yoo, Y.-S. Yu, H. Ha, S. Lee, J.-S. Choi, S. Oh, E. Kang, H. Choi, H. An, K.-S. Lee, J. Y. Park, R. Celestre, M. A. Marcus, K. Nowrouzi, D. Taube, D. A. Shapiro, W. Jung, C. Kim and H. Y. Kim, *Energy Environ. Sci.* 2020, **13**, 1231-1239.

7. P. E. Blöchl, *Phys. Rev. B* 1994, **50**, 17953-17979.

8. G. Henkelman, B. P. Uberuaga and H. A. Jónsson, *J. Chem. Phys.* 2000, **113**, 9901-9904.